The Light Elements and Their Evolution
IAU Symposium, Vol. 198, *2000*
L. da Silva, M. Spite, J. R. de Medeiros, eds.

Creation and Destruction of ^{7}Li and ^{3}He in RGB and AGB Stars

I.-Juliana Sackmann and Arnold I. Boothroyd

W. K. Kellogg Radiation Laboratory 106-38, California Institute of Technology, Pasadena, CA 91125, U.S.A.

Abstract. Early in this decade our theoretical work demonstrated that all AGB stars in the mass range ~ 4 to $\sim 7\,M_\odot$ pass through a stage when a tremendous amount of lithium [up to $\log\varepsilon(^7\mathrm{Li}) \sim 4.5$] is created and transported to the surface. These lithium-rich AGB stars are predicted to occupy a narrow luminosity range between $M_{bol} = -6$ and -7, in excellent agreement with the observations of Smith & Lambert (1989), and might be useful as approximate standard candles. Recently, we found that even low mass stars (~ 1 to $\sim 2\ M_\odot$) on the RGB could create a tremendous amount of surface lithium. In both the AGB and RGB cases, it is the Cameron-Fowler mechanism that is responsible for the lithium creation.

In the AGB stars, it is *hot bottom burning* (nuclear burning at the base of the convective envelope) that produces the lithium. In the RGB stars, it is "*cool bottom processing*" that can lead to either lithium production or destruction. Cool bottom processing results when extra mixing (presumably rotation-induced) transfers material from the cool convective envelope down to the outer wing of the hydrogen-burning shell (where nuclear reactions can take place) and back out to the envelope. If the extra mixing is slow, ^{7}Li is destroyed; if it is fast enough, then ^{7}Li is created — for sufficiently fast and deep extra mixing, $\log\varepsilon(^7\mathrm{Li}) \sim 4$ is possible.

Unlike ^{7}Li, the ^{3}He abundance is almost independent of the mixing speed, and is constrained by observations of $^{12}\mathrm{C}/^{13}\mathrm{C}$ or [C/Fe] on the RGB. Cool bottom processing causes low mass stars of sub-solar metallicity to be net destroyers of ^{3}He, rather than net producers. This is in contrast to previous theoretical predictions, and has a far-reaching effect on our understanding of galactic chemical evolution of ^{3}He.

1. Introduction

Lithium burns at only a few million degrees K; thus the story of lithium in stars has traditionally been one of destruction. Lithium is destroyed during the pre-main sequence evolution by some low mass stars ($M \lesssim 1.2\ M_\odot$ for Population I); it is also observed to be destroyed during the main sequence evolution of low mass stars ($M \lesssim 2\ M_\odot$). Surface lithium abundances are diluted by two orders of magnitude in all low and intermediate mass stars when they reach the lower RGB (due to first dredge-up). According to classical stellar evolution theory, these reduced lithium abundances were not expected to change much subsequent to the RGB stage. On the other hand, as early as 1940, the AGB star WZ Cas was discovered to be superrich in lithium (McKellar 1940). In the next three decades, a handful of other superrich lithium stars were discovered in our galaxy. Some of these stars have lithium abundances orders of magnitude above that of the interstellar medium from which they were born (see, e.g., Wallerstein & Conti 1969; Boesgaard 1970; Abia et al. 1991). All of the superrich lithium stars discovered during this period were AGB stars. Furthermore, in the Magellanic Clouds, lithium enrichment has been discovered in the AGB stars in the magnitude range $-6 \gtrsim M_{bol} \gtrsim -7$ (Smith & Lambert 1989, 1990). Such lithium creation in AGB stars can be understood in terms of "hot bottom burning" (HBB) in intermediate mass stars of $4-7\,M_{\odot}$ (Sackmann, Smith, & Despain 1974; Scalo, Despain, & Ulrich 1975; Sackmann & Boothroyd 1992), as will be discussed in § 3.

In the last two decades, stars rich in lithium have also been discovered on the RGB, starting with the work of Wallerstein & Sneden (1982). In fact, observations indicate that a few percent of all RGB stars are unusually lithium-rich (Brown et al. 1989). A few RGB stars have even been discovered to be superrich in lithium, with abundances above that of the interstellar medium (see, e.g., da Silva, de la Reza, & Barbuy 1995). About 20 lithium-rich RGB stars were discovered by the Pico dos Dias (PDS) Survey, which was searching for T Tauri candidates selected by means of the IRAS Point Source Catalog (Gregorio-Hetem et al. 1992); the fact that most lithium-rich RGB stars show a far-infrared excess (Gregorio-Hetem et al. 1993) suggests a connection between lithium enrichment and mass loss (de la Reza, Drake, & da Silva 1996). These lithium-rich RGB stars appear to have relatively low mass, of order $1-2.5\,M_{\odot}$ (in contrast to the intermediate masses, $4-7\,M_{\odot}$, of the lithium-rich AGB stars). Such lithium creation in RGB stars can be understood in terms of "cool bottom processing" (CBP) in low mass stars (Sackmann & Boothroyd 1999), as will be discussed in § 4.

As far as ^{3}He is concerned, stars were traditionally considered to be net sources of this isotope. Rich pockets of ^{3}He are built up outside the cores of low and intermediate mass stars during their main sequence evolution; subsequently, during the early RGB stage, first dredge-up mixes ^{3}He from this pocket to the surface. High mass stars do not have time to build up a significant ^{3}He-pocket, and a reduction in surface ^{3}He results as first dredge-up reaches into ^{3}He-depleted layers further in. However, the ejecta from low and intermediate mass stars far outweighs the ejecta from the less common high mass stars. Thus, in classical stellar evolution, stars were predicted to strongly enrich the interstellar medium in ^{3}He. This conclusion is dramatically altered when cool bottom processing on the RGB is taken into account, as will be shown in § 4.

2. The Cameron-Fowler Mechanism

Cameron (1955) noted that a significant amount of ^{7}Be could be produced by the $^3\mathrm{He}+\alpha$ reaction in the p-p chain; he also noted that the half-life for electron capture of ^{7}Be is greatly lengthened (to of order 100 years) under stellar interior conditions due to ^{7}Be being almost completely ionized, compared to the 53-day

https://doi.org/10.1017/S0074180900166434 Published online by Cambridge University Press

half-life from K-capture under laboratory conditions. Therefore he reasoned that with the deep convective envelopes of red giants the ^{7}Be would be able to be carried out from the interior regions where it was created to the outer layers before electron capture would take place. The resulting ^{7}Li would thus be created under cool outer-layer conditions, where nuclear burning could not destroy it; it would be observable until the convective currents brought it down to interior layers hot enough for its burning, while at the same time more ^{7}Be was brought up to create new ^{7}Li.

At a jolly party of the Kellogg Radiation Laboratory of Caltech in 1970, Cameron took Willy Fowler aside and told him about the above idea. Willy then added that he had a clue where such a scenario could actually take place. Helium shell flashes (thermal pulses) had just been discovered to take place in AGB stars. Willy suggested that helium shell flashes might occasionally induce complete convection of the outer envelope down to the helium-burning shell. This back-of-the-envelope idea became known thereafter as the Cameron-Fowler mechanism (Cameron & Fowler 1971).

3. Hot Bottom Burning on the AGB

Classical stellar evolution calculations were unable to produce lithium in the surface layers of stars. Classical stellar evolution models did not provide convective envelopes reaching down into high-temperature regions where the $^3\text{He}+\alpha \rightarrow {}^7\text{Be}$ reaction could take place; certainly the "entropy barrier" prevents helium-shell flash convection from joining with the envelope convection (as had been proposed by Cameron & Fowler [1971]). However, Iben (1975) was able to reach high temperatures (60 million K) at the base of the conventional convective envelope of a $7\,M_\odot$ AGB star — hot enough for ^{7}Be production. Despite this fact, he found no lithium production, because he made the classical assumption of *instantaneous* convective mixing (Iben 1973).

Since the early observations of the superrich lithium stars clearly demonstrated that lithium creation did indeed take place in some stars, Sackmann et al. (1974) introduced models with a novel (non-classical) feature: an improved description of convective mixing was introduced, namely, time-dependent "convective diffusion" coupled to nuclear burning, discretized over many layers from the surface to the base of convection. In addition, the assumption was made that the convective envelope penetrated right down into the center of the hydrogen-burning shell, at 50 million K; such deep convective envelopes were not achievable in a self-consistent way at the time. On the other hand, this non-classical calculation *was* able to account for the superrich lithium abundances for the first time. Scalo et al. (1975), using the Sackmann et al. (1974) convective diffusion code in AGB envelope models (with inner boundary conditions estimated from the core mass–luminosity relation), again found high temperatures at the base of the convective envelope (which they christened "hot bottom burning"), together with the lithium production.

It became clear in the 1980's, when improved opacities became available, that the canonical value of unity for the mixing length parameter "α" (the mixing length relative to the pressure scale height) was incorrect; it had to be increased significantly (by about 50 to 100%, depending on the opacities used),

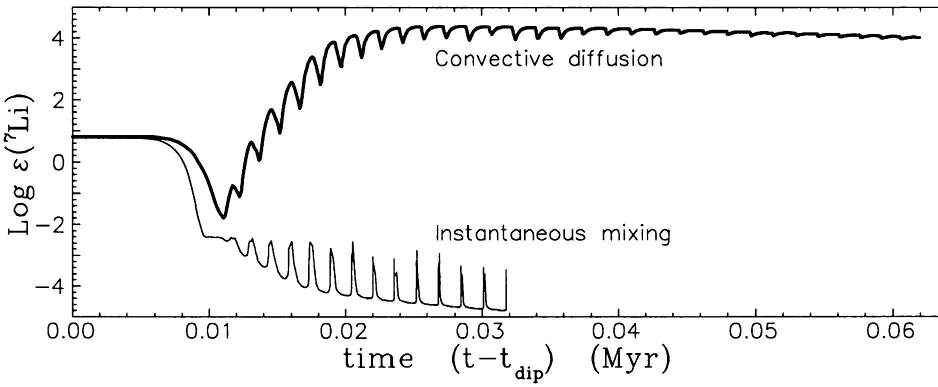

Figure 1. Lithium production in a 6 $M_\odot$, $Z = 0.02$ AGB star, comparing the time-dependent "convective diffusion" mixing algorithm with the "instantaneous mixing" approximation ($t_{\rm dip}$ is the time of the pre-flash luminosity "dip").

e.g., to obtain a correct solar model (Sackmann, Boothroyd, & Fowler 1990) and the correct position of the base of the RGB. Sackmann & Boothroyd (1991) demonstrated that the temperature at the base of the convective envelope on the AGB increases steeply as a function of α, for $1 \lesssim \alpha \lesssim 2$. For AGB stars between about 4 and 7 $M_\odot$, these new opacities and the corresponding larger α values yielded hot bottom burning in the envelopes of stellar models, i.e., in *self-consistent* models (rather than merely being assumed, as in the earlier lithium-production models).

Sackmann & Boothroyd (1992) applied the time-dependent "convective diffusion" algorithm of Sackmann et al. (1974) to the new hot bottom burning AGB models, producing for the first time self-consistent models for ^{7}Li production (shown as a function of time in Figure 1; the wiggles correspond to successive helium shell flashes. Also demonstrated in Figure 1 is the fact that the classical "instantaneous mixing" approximation leads to lithium destruction, rather than creation. Figure 2 is a key diagram, showing the predicted ^{7}Li abundances as a function of AGB luminosity for various stellar masses and metallicities. The peak lithium abundance reached, of $\log \varepsilon(^7\mathrm{Li}) \sim 4.5$, is consistent with the highest lithium abundances observed in galactic superrich lithium stars (Abia et al. 1991; Denn, Luck, & Lambert 1991). Figure 2 illustrates the theoretical prediction that the high ^{7}Li abundances occur in the magnitude range $-6 \gtrsim M_{bol} \gtrsim -7$, in excellent agreement with the Magellanic Cloud observations of Smith & Lambert (1989, 1990). Figure 2 also demonstrates that the peak ^{7}Li abundances are roughly independent of stellar mass and metallicity (for stars in the range $4 - 7\ M_\odot$, where hot bottom burning takes place). Since the magnitude range (where ^{7}Li abundance is high) is relatively narrow, these superrich lithium stars on the AGB can in principal be used as approximate standard candles to yield distances; Ventura, D'Antona, & Mazzitelli (1999) pointed out that considering only the lithium-rich C-stars would work even better, as they have a narrower luminosity range and are less prone to confusion with lithium-rich RGB stars. Figure 2 also illustrates that the ^{7}Li abundance

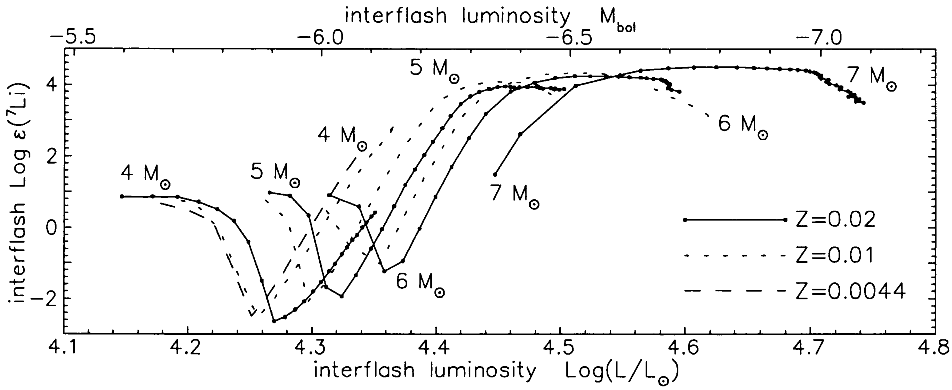

Figure 2. Lithium abundances in hot bottom burning AGB stars as a function of (interflash) luminosity, for various stellar masses at solar metallicity ($Z = 0.02$) and at approximate Large and Small Magellanic Cloud metallicities ($Z = 0.01$ and 0.0044, respectively).

declines as the ^{3}He fuel is used up; this decline continues much further than shown by the truncated runs of Figure 2, and thus these models are consistent with the observed range of abundances in lithium-rich Small Magellanic Cloud AGB stars, namely, $1.9 \lesssim \log \varepsilon(^7\mathrm{Li}) \lesssim 3.5$ (Plez, Smith, & Lambert 1993).

4. Cool Bottom Processing on the RGB

After the excellent agreement between our theoretical predictions of superrich lithium stars on the AGB and the observations of such stars, we were made aware of recent observational discoveries of lithium-rich low-mass stars on the RGB (as summarized, unfortunately too briefly, in § **??**). These lithium-rich RGB stars could *not* be accounted for by our theoretical models, since hot bottom burning does not occur on the RGB (nor does it occur even on the AGB in such low mass stars). To attempt to explain these mysterious lithium-rich RGB stars, we turned to the RGB extra mixing phenomenon that had long been invoked to explain RGB carbon observations. It has been suggested since the 1970's that the anomalously low ^{12}C/^{13}C ratios observed in low mass RGB stars could be accounted for by extra mixing below the convective envelope, which could convert ^{12}C into ^{13}C (see, e.g., Dearborn, Eggleton, & Schramm 1976; Sweigart & Mengel 1979). The term "cool bottom processing" (CBP) for this extra mixing with nuclear processing was coined by Wasserburg, Boothroyd, & Sackmann (1995); the difference between hot bottom burning and cool bottom processing is illustrated schematically in Figure 3.

First dredge-up leaves behind a composition discontinuity in the star, with a steep molecular weight gradient, frequently referred to as the "μ-barrier"; this μ-barrier is strongly stable against mixing, acting like a wall. RGB observations of Population I stars and field Population II stars indicate that the extra mixing region cannot reach from the convective envelope into the neighborhood of the hydrogen-burning shell until the hydrogen-burning shell has reached and de-

https://doi.org/10.1017/S0074180900166434 Published online by Cambridge University Press

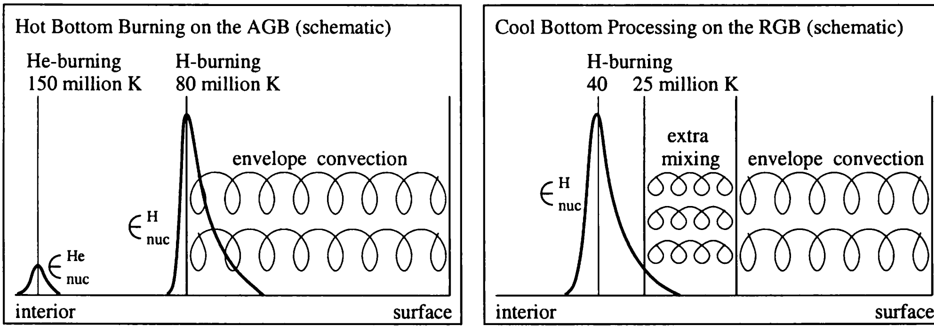

Figure 3. Schematic illustration of the difference between *hot bottom burning* and *cool bottom processing*; typical temperatures are shown.

stroyed this intervening μ-barrier (see, e.g., Charbonnel 1994; Charbonnel 1995; Boothroyd & Sackmann 1999). On the other hand, it is noteworthy that the extra mixing does appear to be able to penetrate this μ-barrier in globular cluster RGB stars, as discussed in Boothroyd & Sackmann (1999).

Charbonnel (1995) showed that extra mixing could lead to lithium *destruction* in low-mass RGB stars of low metallicity, explaining the anomalously *low* lithium abundances that are observed late on the RGB in in field Population II stars. Sackmann & Boothroyd (1999) demonstrated for the first time that cool bottom processing on the RGB could also lead to lithium *creation*. The extra mixing was assumed to reach into the outer wing of the hydrogen-burning shell, and was modelled as a "conveyer-belt" type circulation. As shown in Figure 4, a relatively long-lived mixing "episode" was modelled in a solar-mass Population I star at an RGB luminosity $\log L = 1.5$ (i.e., at the stage on the RGB where the hydrogen-burning shell has just reached and destroyed the μ-barrier): the extra mixing was assumed to reach down to within $\Delta \log T = 0.17$ of the bottom of the hydrogen-burning shell, and was assumed to last long enough to reproduce the observed RGB $^{12}C/^{13}C$ ratio of ~ 11 (namely, lasting 12.5 million years — short compared to the RGB evolutionary timescale). The left-hand panel of Figure 4 illustrates, for a circulation speed of $10^{-3}\ M_\odot/\text{yr}$, the lithium production reaching as high a value as $\log \varepsilon(^7\text{Li}) \sim 3$ for a period of $\sim 10^6$ yr, after which the lithium abundance declines due to its ^{3}He fuel being used up, as shown in the figure. Different speeds of circulation were considered; the right-hand panel of Figure 4 illustrates the strong sensitivity of the lithium abundance to the mixing speed. It demonstrates that rapid mixing speeds ($\gtrsim 10^{-4}\ M_\odot/\text{yr}$, in this model) lead to lithium creation, while slower mixing leads to lithium destruction. The upper limit to the speed of this extra mixing is that it should be much slower than convective mixing, which has a speed of order $1\ M_\odot/\text{yr}$ in RGB envelopes; the lower limit is the requirement that the mixing be faster than the speed with which the hydrogen shell burns its way outwards (of order $10^{-8}\ M_\odot/\text{yr}$ for the above model).

Figure 5 illustrates a different ("continuous") extra mixing scenario, where circulation was assumed to start when the μ-barrier was destroyed and to continue until the tip of the RGB was reached, but always reaching the same

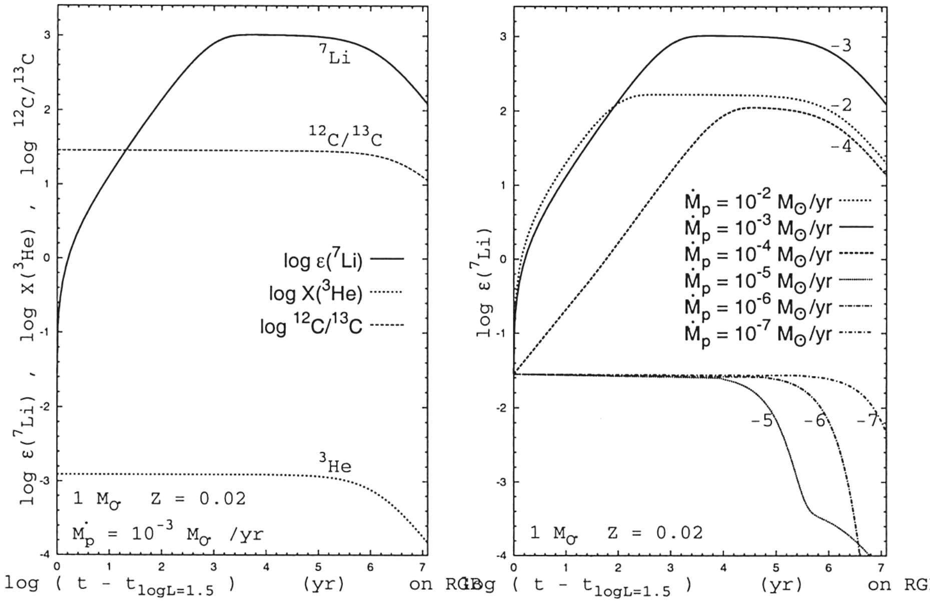

Figure 4. Lithium production as a function of time on the RGB, for a circulation model of a long-lasting extra mixing episode.

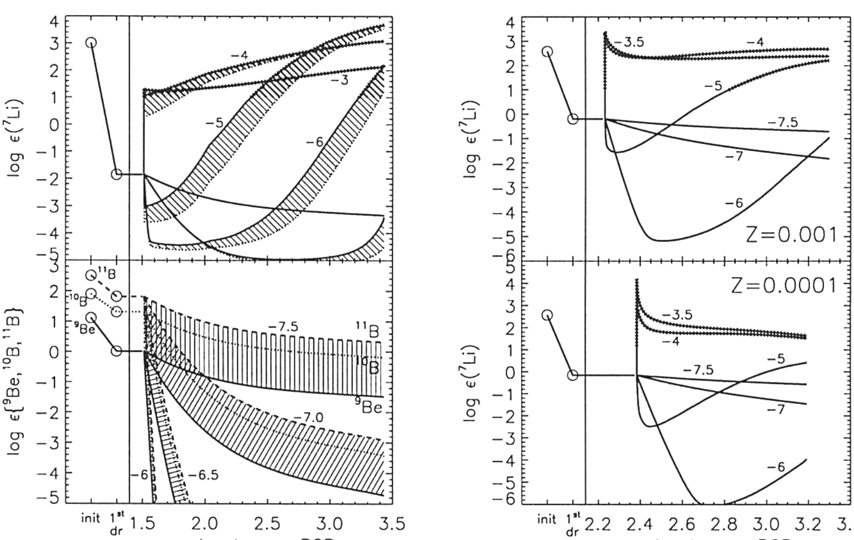

Figure 5. Lithium production as a function of RGB luminosity, for a "continuous" model where extra mixing continues to the end of the RGB.

https://doi.org/10.1017/S0074180900166434 Published online by Cambridge University Press

distance in temperature from the base of the hydrogen-burning shell, namely, $\Delta \log T = 0.26$, in order to reproduce the observed RGB $^{12}C/^{13}C$ ratio of ~ 11 by the time the star reached the tip of the RGB. Figure 5 shows the lithium creation and destruction from such a model in a $1\, M_\odot$ star as it climbs the RGB. The upper left-hand panel illustrates that, for most mixing speeds, such continuous mixing leads to the highest lithium abundances near the tip of the RGB; for a mixing speed of $\sim 10^{-4}\ M_\odot/\mathrm{yr}$, $\log \varepsilon(^7\mathrm{Li}) \sim 4$ can be attained. Note the switchover between lithium creation and destruction as one changes the mixing speed. The shaded areas show the effect of changing the circulation geometry, as discussed in detail in Sackmann & Boothroyd (1999). The lower left-hand panel illustrates that the stable beryllium and boron isotopes are rapidly depleted, except at the very lowest mixing speeds; shaded areas tie together abundance curves for a given mixing speed. The right-hand panel of Figure 5 illustrates this "continuous" circulation model (with the same $\Delta \log T = 0.26$) for Population II objects. At all but the very slowest mixing speeds, the ^{3}He is largely destroyed soon after extra mixing begins, due to the higher temperature of the hydrogen-burning shell in Population II RGB stars. As a consequence, the highest attainable lithium abundances $\log \varepsilon(^7\mathrm{Li}) \sim 4$ are attained shortly after extra mixing starts on the RGB (rather than at the tip of the RGB), but only for rapid mixing speeds $\gtrsim 10^{-4}\ M_\odot/\mathrm{yr}$; lower but still observable amounts of lithium are maintained thereafter. Mixing speeds of $\sim 10^{-5}\ M_\odot/\mathrm{yr}$ lead first to destruction, then to creation of observable amounts of lithium near the RGB tip; slower mixing speeds lead only to lithium destruction.

The RGB carbon observations suggest an extra mixing scenario in between the above two mixing scenarios; presently, lithium observations may point towards a number of short successive mixing episodes (de la Reza et al. 1996).

5. Creation and Destruction of ^{3}He

Figures 6 and 7 illustrate the creation and destruction of ^{3}He as a function of stellar mass, for Population I and II stars, respectively. First dredge-up leads to considerable envelope enrichment of ^{3}He in low mass stars, and slight depletion in higher mass stars ($\gtrsim 5 M_\odot$); see also § **??**. In low mass stars ($\lesssim 2\, M_\odot$), cool bottom processing subsequently on the RGB destroys ^{3}He, and thus low mass stars of sub-solar metallicity are *not* sources of ^{3}He enrichment in the interstellar medium; Population II stars destroy much more ^{3}He than Population I stars. The amount of ^{3}He destruction due to CBP is uncertain by a factor of about 2; the strongest constraint is provided by observations of $^{12}C/^{13}C$ and [C/Fe] on the RGB, which constrain the total amount of processing, but the ^{3}He-burning reactions have a different temperature dependence from the CN-cycle rates, and thus the temperature at which the processing takes place has some effect on the amount of ^{3}He-burning associated with a given (observed) amount of CN-cycle processing. However, it is clear from Figure 7 that CBP in low mass Population II stars destroys essentially all their ^{3}He. Second dredge-up on the early AGB has only a relatively minor effect. For stars between ~ 4 and $7\, M_\odot$, hot bottom burning on the AGB will destroy essentially all the ^{3}He that is present.

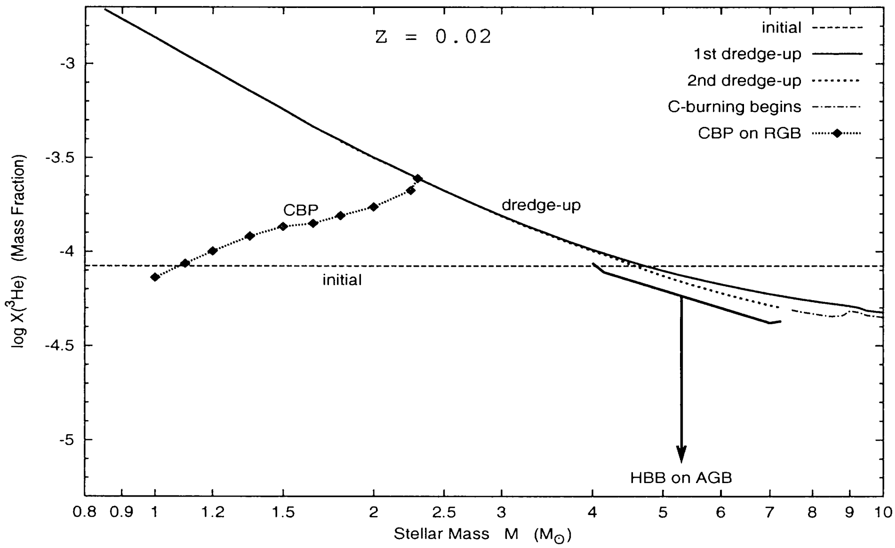

Figure 6. Production and depletion of ^{3}He in Population I stars. Heavy black diamonds show an estimate of the destruction of ^{3}He due to cool bottom processing (CBP), relative to the first dredge-up value. Bracket with arrow shows the mass region where hot bottom burning (HBB) on the AGB destroys the ^{3}He.

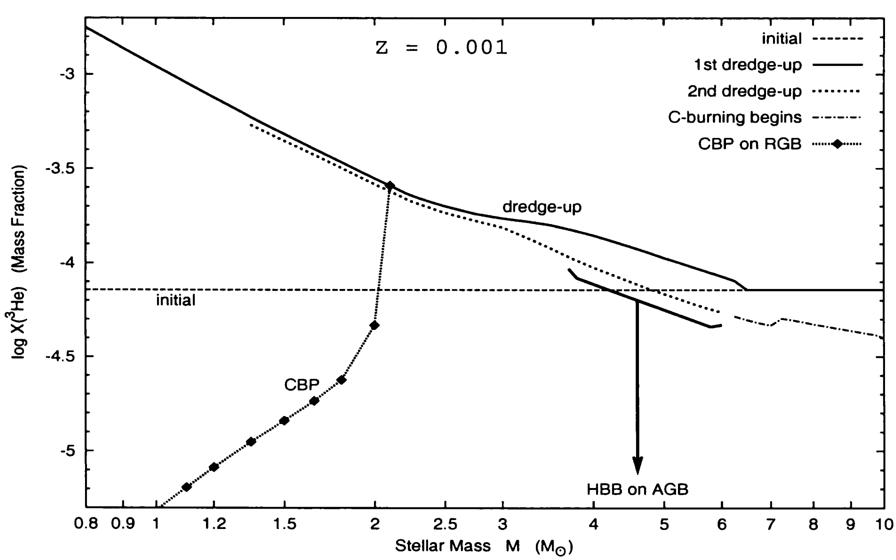

Figure 7. Production and depletion of ^{3}He in Population II stars; symbols as in Fig. 6.

https://doi.org/10.1017/S0074180900166434 Published online by Cambridge University Press

Acknowledgments. We wish to acknowledge helpful discussions with C. A. Barnes and the support of R. D. McKeown of the Kellogg Radiation Laboratory. This work was partially supported by a grant from NSF PHY-9420470. One of us (I.-J. S.) wishes to acknowledge partial travel support to the Natal meeting from T. A. Tombrello, Division Chairman of Physics, Mathematics, and Astronomy of the California Institute of Technology.

References

Abia, C., Boffin, H. M. J., Isern, J., & Rebolo, R. 1991, ApJ, 245, L1

Brown, J. A., Sneden, C., Lambert, D. L., & Dutchover, E., Jr. 1989, ApJS, 71, 293

Boesgaard, A. M. 1970, ApJ, 161, 1003

Boothroyd, A. I., & Sackmann, I.-J. 1999, ApJ, 510, 232

Cameron, A.G.W. 1955, ApJ, 121, 144

Cameron, A.G.W., & Fowler, W. A. 1971, ApJ, 164, 111

Charbonnel, C. 1994, A&A, 282, 811

Charbonnel, C. 1995, ApJ, 453, L41

Dearborn, D., Eggleton, P. P., & Schramm, D. N. 1976, ApJ, 203, 455

da Silva, L., de la Reza, R., & Barbuy B. 1995, ApJ, 448, L41

de la Reza, R., Drake, N. A., & da Silva, L. 1996, ApJ, 456, L115

Denn, G. R., Luck, R. E., & Lambert, D. L. 1991, ApJ, 377, 657

Gregorio-Hetem, J., Castilho, B. V., & Barbuy, B. 1993, A&A, 268, L25

Gregorio-Hetem, J., Lépine, J. R. D., Quast, G. R., Torres, C. A. O., & de la Reza, R. 1992, AJ, 103, 549

McKellar, A. 1940, PASP, 52, 407

Iben, I., Jr. 1973, ApJ, 185, 209

Iben, I., Jr. 1975, ApJ, 196, 525

Plez, B., Smith, V. V., & Lambert, D. L. 1993, ApJ, 418, 812

Sackmann, I.-J., & Boothroyd, A. I. 1991, ApJ, 366, 529

Sackmann, I.-J., & Boothroyd, A. I. 1992, ApJ, 392, L71

Sackmann, I.-J., & Boothroyd, A. I. 1999, ApJ, 510, 217

Sackmann, I.-J., Boothroyd, A. I., & Fowler, W. A. 1990, ApJ, 360, 727

Sackmann, I.-J., Smith, R. L., & Despain, K. H. 1974, ApJ, 187, 555

Scalo, J. M., Despain, K. H., & Ulrich R. K. 1975, ApJ, 196, 805

Smith, V. V., & Lambert, D. L. 1989, ApJ, 345, L75

Smith, V. V., & Lambert, D. L. 1990, ApJ, 361, L69

Sweigart, A. V., & Mengel, J. G. 1979, ApJ, 229, 624

Ventura, P., D'Antona, F., & Mazzitelli, I. 1999, ApJ, 524, L111

Wallerstein, G. & Conti, P. S. 1969, ARA&A, 7, 99

Wallerstein, G. & Sneden, C. 1982, ApJ, 255, 577

Wasserburg, G. J., Boothroyd, A. I., & Sackmann, I.-J. 1995, ApJ, 447, L37